Impurity induced magnetism in graphene

A Project Report

submitted by

SYED SAJID ALI | EE11B104

in partial fulfilment of the requirements

for the award of the degree of

BACHELOR OF TECHNOLOGY AND MASTER OF TECHNOLOGY

DEPARTMENT OF ELECTRICAL ENGINEERING
INDIAN INSTITUTE OF TECHNOLOGY MADRAS.

June 2016

THESIS CERTIFICATE

This is to certify that the thesis titled **Impurity induced magnetism in graphene**, submitted by **Sajid Ali**, to the Indian Institute of Technology, Madras, for the award of the degree of **Master of Technology**, is a bona fide record of the research work done by him under our supervision. The contents of this thesis, in full or in parts, have not been submitted to any other Institute or University for the award of any degree or diploma.

Prof. Ranjit Nanda
Research Guide
Assistant Professor
Dept. of Physics
IIT-Madras
Chennai 600 036

Place: Chennai

Date: 10 June 2016

ACKNOWLEDGEMENTS

I would like to thank Prof. B.R.K. Nanda for having given me a chance to work with him and hence to explore graphene and for guidance that he provided me throughout the course of the project.

I would also like to thank both current and former members of the Condensed Matter Theory and Computational Lab at IIT Madras for help with learning to perform dft calculations and providing valuable support.

ABSTRACT

KEYWORDS: Graphene; intercalation; magnetism

Using density functional calculations we explore the possibilities of inducing spin moments in otherwise non-magnetic electronic structure of monolayer and bilayer graphene by introducing impurities. We follow two approaches for this. In the first approach, we attach hydrogen atoms to carbon atoms on monolayer graphene at varying densities. In the second approach, we intercalate H, N, O and F atoms between the two layers of graphene. We introduce another layer of atoms between the two grahene layers as a possible method to stabilize the intercalated atom while preserving the magnetism.

TABLE OF CONTENTS

LIST OF TABLES

LIST OF FIGURES

ABBREVIATIONS

DFT	Density Functional Theory
SCF	Self Consistent Field
QE	Quantum Espresso
MLG	Monolayer graphene
BLG	Bilayer graphene
LDA	Local Density Approximation
GGA	Generalized Gradient Approximation
DOS	Density of states

NOTATION

n(r)	Electron Density
ecutwfc	kinetic energy cutoff in Ry

CHAPTER 1

Introduction and Methodology

1.1 Introduction

Information processing and storage based technologies are rapidly reaching their limits. As the transistor, the basic component behind today's microprocessor gets small enough to the point where the channel is just a couple of atoms wide, quantum effects become important. This points to a pressing need for development of new technologies that embrace the quantum nature of electron.

Studying magnetism can help us in taking advantage of spin of the electron. Spintroncis promises faster and more energy efficient devices[1]. In this thesis, we study magnetism from a materials viewpoint. We map out the different methods by which a magnetic moment can be induced in graphene with the aim of using graphene in spintronic devices.

Monolayer graphene has been the focus of active research ever since it was discovered [2],[3]. Due to its unusual band structure and extremely high conductivity it has been suggested that it could be used in wide ranging applications[4]. Bilayer graphene has a band gap, which is not present in monolayer graphene. The absence of band gap has prevented the use of graphene as a semiconductor for transistors as it had a very low on/off ratio[5].

Graphene is a promising material for spintronics applications due to high electron mobility which aids in achieving spin coherence over microns, low spin-orbit coupling and weak hyperfine interactions between electron spin and carbon nuclei[6]. Recently, the spin hall effect was demonstrated in hydrogenated graphene occurring due to the enhancement of spin-orbit coupling[7].

Pristine graphene is strongly diamagnetic[8]. Inducing magnetic moments in graphene and/or its bilayer is the first step towards making graphene magnetic. Once these moments are created, attempts can be made at achieving ordering. If achieved it can open the door to many applications spintronics[9].

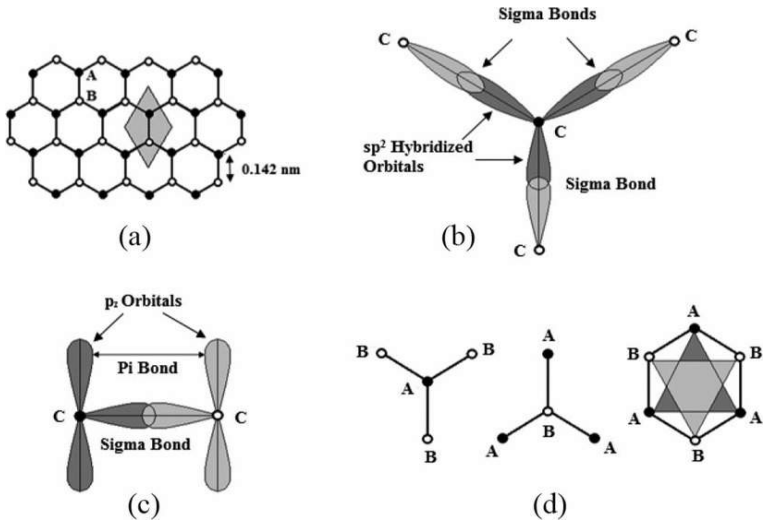

Figure 1.1: Structure of graphene. (a) Honeycomb lattice of carbon atoms, the dark circles and the unfilled circles represent carbon atoms at two different sites designated respectively as A and B, the shaded region indicates a unit cell. (b) sp Formula hybridized orbitals of carbon atoms symmetrically distributed in the molecular plane at angles of 120° forming three Formula-bonds with those of the three nearest neighbors. (c) Orbitals of the remaining electrons distributed perpendicular to the molecular plane form Formula-bonds with those of one of the nearest neighbor, assigning four bonds to each carbon atoms. (d) Two different orientations of the arrangement of carbon atoms at lattice sites A and B, the honeycomb lattice can be viewed as two interpenetrating triangular lattices of A and B carbon atoms.[20]

There have been many theoretical, computational and experimental studies that have attempted to make graphene and/or its bilayer version magnetic by the clever use of defects. These include: use of magnetic adatoms[10], use of vacancies[11],[12],[13], functionalization through hydrogenation[14], aryl radicals[15], proximity induced magnetism[16], etc . There has been experimental observation of ferromagnetism in hydrogenated monolayer graphene[14],[17].

A brief review of the literature suggests that the functionalization of graphene to induce magnetism is primarily associated with the adsorption of functional groups on the graphene plane[15]. In these cases the electron-hole symmetry of graphene is broken to induce carbon magnetism [18],[19].

1.2 Density Functional Theory

Density functional theory is a popular computational method to solve the many-body Schroedinger equation which is exact in theory, but approximate in practice [1]. The ground state density $\mathbf{n}_o$(r), determines the properties of the ground state. Any property of the system can be viewed as a functional of the ground state density. The ground state electronic density $\mathbf{n}_o$(r) can be found by minimizing E[**n**], which gives the energy of the system[21].

$$H_{tot} = -\frac{h^2}{2\mathrm{m}_e}\sum_i \nabla_i^2 - \sum_{i,I}\frac{Z_I e^2}{|r_i - R_J|} + \frac{1}{2}\sum_{i\neq j}\frac{e^2}{|r_i - r_j|} - \sum_I \frac{h^2}{2M_I}\nabla_I^2 + \frac{1}{2}\sum_{I\neq J}\frac{Z_I Z_J e^2}{|R_I - R_J|} \tag{1.1}$$

Many Body Schroedinger equation where the first term represents the kinetic energy of electrons, the second term represents the interaction between electrons and the nuclei, the third term represents interactions between electrons, the fourth term represents the kinetic energy of the nuclei and the fifth term represents the interactions between the nuclei. The schrodinger equation is not analytically solvable for more atoms with more than one electron necessitating the need to develop approximate methods, with DFT being one of them.

[1] This section is based upon Electronic Structure by Richard M Martin

1.2.1 Hohenberg-Kohn Theorems

The basis of the technique was laid down by Hohenberg and Kohn who in 1964 showed that the ground state density can be treated as a basic variable and that all properties of the system can be derived from it.[21][22]. The theorems are:

(1) For any system of interacting particles in an external potential, $V_{ext}(r)$, the potential $V_{ext}(r)$ is determined uniquely, except for a constant by the ground state particle density.

(2) A universal functional for the energy E[**n**] in terms of the density $\mathbf{n}_o$ can be defined, valid for any external potential $V_{ext}(r)$. For a particular $V_{ext}(r)$, the exact ground state energy of the system is the global minimum value of this functional, and the density **n**(r) that minimizes the functional is the exact ground state density $\mathbf{n}_o(r)$.

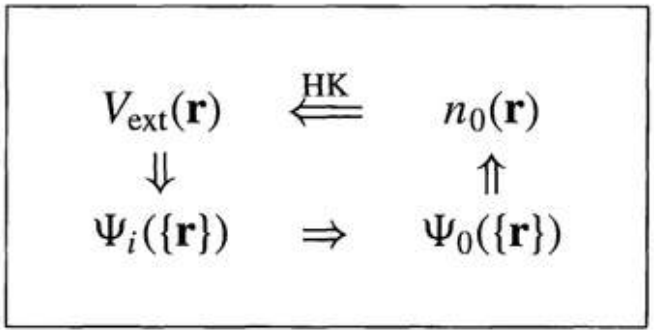

Figure 1.2: Hohenberg Kohn Theorem : Given any external potential, Schrodinger equation determines all the possible states which includes the ground state and Hohenberg Kohn theorem places a one to one correspondence between this ground state density and the external potential[21]

These theorems were proved by Hohenberg and Kohn[22], but did not offer a way to find the functionals. These theorems were later extended to include dependency on spin[23] and for finite temperatures[24].

1.2.2 Kohn-Shan Theorems

Kohn and Sham in 1965[25] proposed an ansatz to perform exact calculations on many body systems using the insight of Hohenberg and Kohn. The ansatz was to replace the

original interacting many body problem by an independent particle problem, the ground state density of which is equal to our original system.

The Kohn Sham energy functional is :

$$E_{KS} = T_s[\mathbf{n}] + \int d\mathbf{r} \mathbf{V}_{ext}(r)\mathbf{n}(r) + E_{Hartree}[\mathbf{n}] + E_{11} + E_{xc}[\mathbf{n}] \tag{1.2}$$

where,

$$\mathbf{n}(r) = \sum_{\sigma} \sum_{i=1}^{N^\sigma} |\psi_i^\sigma(r)|^2 \tag{1.3}$$

represents the density,

$$T_s = -\frac{1}{2} \sum_{\sigma} \sum_{i=1}^{N^\sigma} < \psi_i^\sigma(r)|\nabla^2|\psi_i^\sigma(r) >= \frac{1}{2} \sum_{\sigma} \sum_{i=1}^{N^\sigma} \int d^3\mathbf{r} |\nabla \psi_i^\sigma(r)|^2 \tag{1.4}$$

represents the kinetic energy,

$$E_{Hartree}[\mathbf{n}] = \frac{1}{2} \int d^\mathbf{r} d^{\mathbf{r}'} \frac{n(r)n(r')}{|r - r'|} \tag{1.5}$$

represents the energy of electron electron interaction,

E_{11} represents the interaction between the nuclei, V_{ext}(r) is the potential due to nuclei and any external fields, and all the exchange and correlation effects are captured in E_{xc} which has to be approximated.

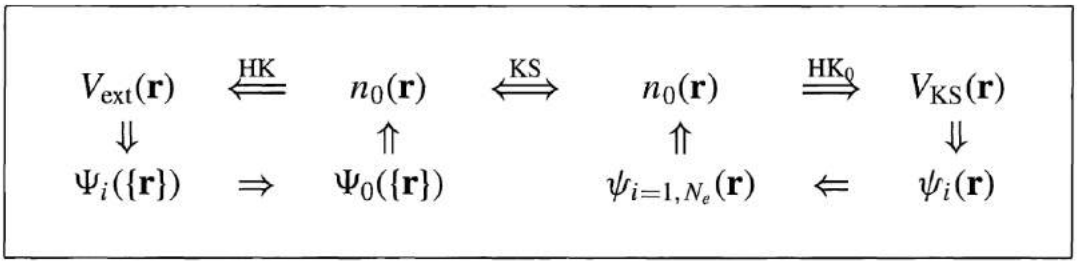

Figure 1.3: Kohn Sham ansatz relating the original many body system to a system of non-interacting particles[21]

1.2.3 Kohn-Shan variational equations

The variational Kohn Sham equations are :

$$\frac{\delta E_{KS}}{\delta \psi_i^{\sigma *}(r)} = \frac{\delta T_S}{\delta \psi_i^{\sigma *}(r)} + [\frac{\delta E_{ext}}{\mathbf{n}(r,\sigma)} + \frac{\delta E_{Hartree}}{\mathbf{n}(r,\sigma)} + \frac{\delta E_{xc}}{\mathbf{n}(r,\sigma)}] * \frac{\mathbf{n}(r,\sigma)}{\delta \psi_i^{\sigma *}(r)} \tag{1.6}$$

where:

$$\frac{\delta T_S}{\delta \psi_i^{\sigma *}(r)} = -\frac{1}{2}\nabla^2 \delta \psi_i^{\sigma}(r) \tag{1.7}$$

and

$$\frac{\mathbf{n}(r,\sigma)}{\delta \psi_i^{\sigma *}(r)} = \psi_i^{\sigma}(r) \tag{1.8}$$

which leads to

$$(H_{KS}^{\sigma} - \epsilon_i^{\sigma})\delta \psi_i^{\sigma(r)} = 0 \tag{1.9}$$

The effective Kohn Sham hamiltonian,

$$H_{KS} = -\frac{1}{2}\nabla^2 + V_{KS}^{\sigma}(r) \tag{1.10}$$

with

$$V_{KS} = V_{ext}(r) + \frac{\delta E_{Hartree}}{\mathbf{n}(r,\sigma)}] + \frac{\delta E_{xc}}{\mathbf{n}(r,\sigma)}] \tag{1.11}$$

$$= V_{ext}(r) + V_{Hartree}(r) + V_{xc}(r) \tag{1.12}$$

Kohn Sham equations are solved self - consistently as show below :

The most common approximation for $E_{xc}[\mathbf{n}]$ is the local density approximation (LDA) and it has the following form :

$$E_{xc}^{LDA} = \int \rho(r)\epsilon_{xc}(\rho(r))dr \tag{1.13}$$

The other most common approximation takes into account the gradient of the density along with the density itself and is called generalized gradient approximation (GGA).

$$E_{xc}^{GGA} = \int \rho(r)\epsilon_{xc}(\rho(r), \nabla\rho(r))dr \tag{1.14}$$

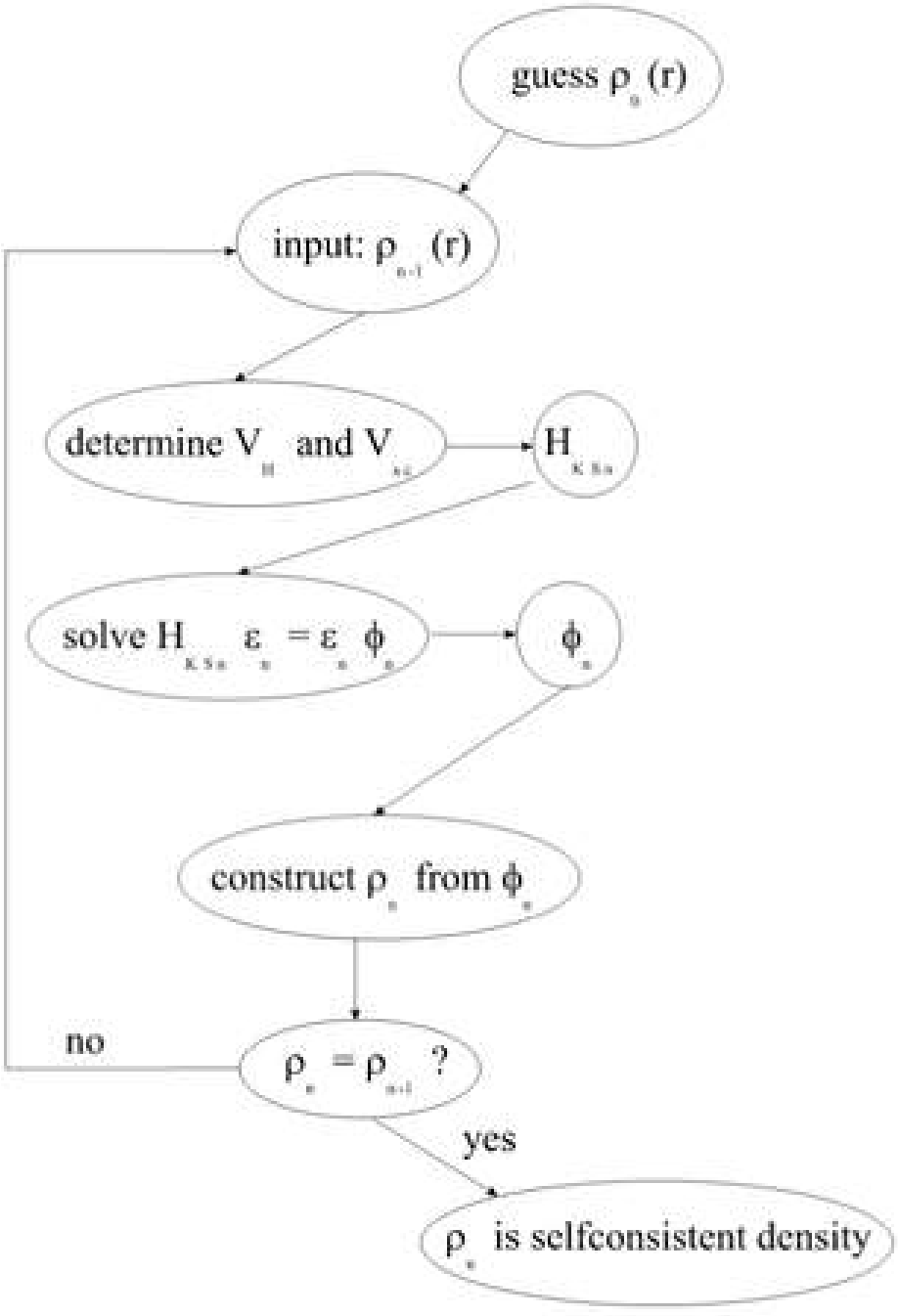

Figure 1.4: Self consistent solution of Kohn - Sham equations[26]

1.2.4 Plane wave basis set

The Kohn Sham equations can be solved in a number of basis sets : atomic basis, plane waves, augmented plane waves, gaussian basis etc. We will be concentrating on plane wave basis set here. Plane wave basis sets are orthogonal, independent of atomic positions and no optimization is needed while using the basis set on different systems. But the drawback being that a large number of basis sets are required. To get around this issue, pseudo potentials are used where the inner or core electrons are frozen and only valence electrons are considered.

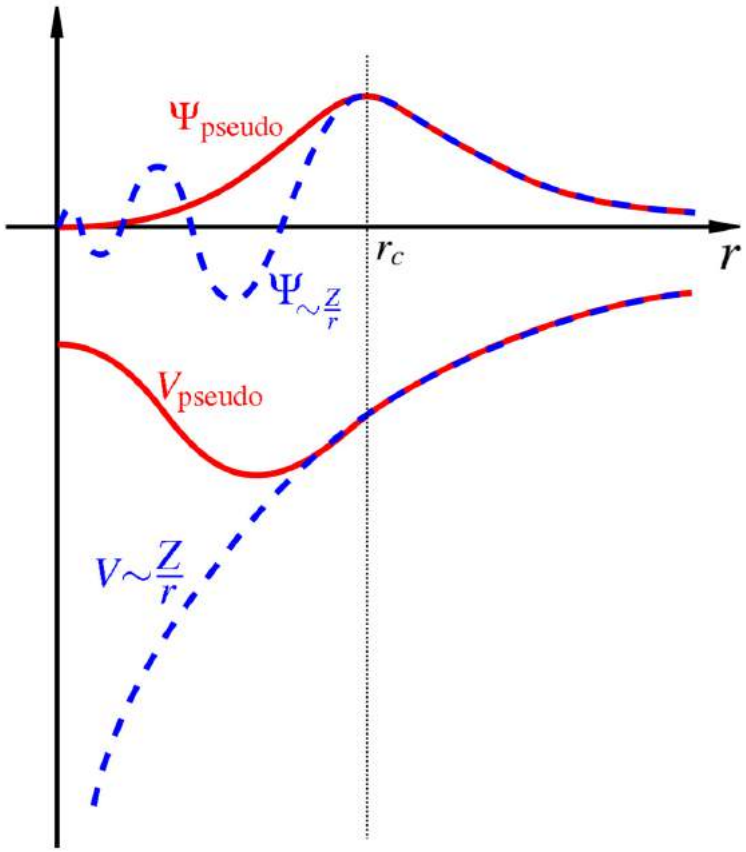

Figure 1.5: Wavefunction in pseudopotential(red) vs coulomb potential(blue)[27]

The wave function is thus described as :

$$\psi_{\vec{k}}^{n}(\vec{r}) = \sum_{\vec{K}} c_{\vec{K}}^{n,\vec{K}} \exp i(\vec{k}+\vec{K}).\vec{r} \tag{1.15}$$

where the basis functions are :

$$|\vec{K}> = \exp i(\vec{k}+\vec{K}).\vec{r} \tag{1.16}$$

In theory, the plane wave basis contains infinite elements, but in practice a cut-off energy is used to limit the size of the basis set. The cut off energy E_{cut} relates to a reciprocal space vector K_{max} and all $\vec{K}$ inside the sphere with radius K_{max} are taken as the basis. The cut off energy is calculated as :

$$E_{cut} = \frac{h^2 K_{max}^2}{2m_e} \tag{1.17}$$

This plane wave basis is used to solve the Kohn Sham equations at k-points that sample the brillouin zone effectively. A popular scheme to sample the brillouin zone is Monkhorst-Pack.

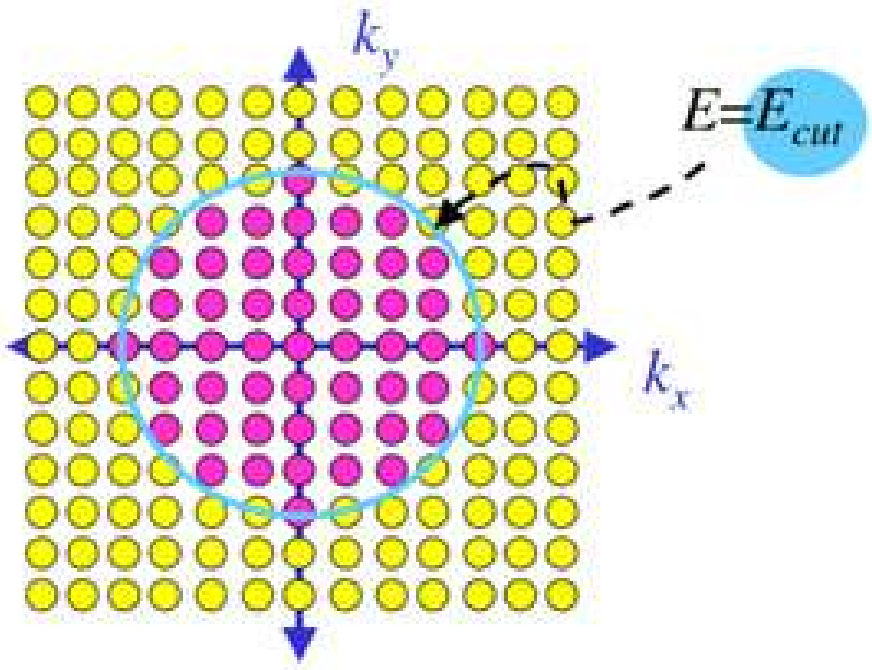

Figure 1.6: The energy cut off[28]

1.3 Thesis overview

While vacancies in monolayer graphene give rise to magnetic moment, controlling thier formation remains a challenge as this requires us to manage the resultant stress. In this thesis, we study alternative methods to produce magnetic moments namely functionalizaztion and intercalation. In Chapter 2, we present out work on functionalization of monolayer graphene. In Chapter 3, we present out work on impurity intercalation in

bilayer graphene. In Chapter 4, we present our work on force analysis of intercalated atoms in bilayer graphene. Also, we discuss possible ways of stabilizing them.

REFERENCES

[1] Igor Zutic, Jaroslav Fabian, S. Das Sarma *Rev. Mod. Phys.* **76** 323 (2004)

[2] K.S. Novoselov, A.K. Geim, S.V. Morozov, D. Jiang, Y. Zhang, S.V. Dubonos, I.V. Grigorieva, A.A. Firsov, *Science* **306** 5696 (2004)

[3] *Nature Nanotechnology* **5** 755 (2010)

[4] A.H. Castro Neto, F. Guinea, N.M.R. Peres, K.S. Novoselov, A.K. Geim *Rev. Mod. Phys.* **81** 109 (2009)

[5] Frank Schwierz *Nature Nanotechnology* **5** 487 - 496 (2010)

[6] Tombros N, Jozsa C, Popinciuc M, Jonkman HT, van Wees BJ, *Nature* **448**7153 (2007)

[7] Jayakumar Balakrishnan, Gavin Kok Wai Koon, Manu Jaiswal, A.H. Castro Neto, Barbaros Ozyilmaz, *Nature Physics* **9** 284 - 287 (2013)

[8] M. Sepioni, R.R. Nair, S. Rablen, J. Narayanan, F. Tuna, R. Winpenny, A.K. Geim, I.V. Grigorieva *Phys. Rev. Lett.* **105** 207205 (2010)

[9] Wei Han, Roland K. Kawakami, Martin Gmitra, Jaroslav Fabian *Nature Nanotechnology* **9** 794 - 807 (2014)

[10] E.J.G. Santos, D. Sanchez-Portal, A. Ayuela *Phys. Rev. B* **81** 125433 (2010)

[11] Oleg V. Yazyev and Lothar Helm *Phys. Rev. B* **75** 125408 (2007)

[12] R.R. Nair, M. Sepioni, I-Ling Tsai, O. Lehtinen, J. Keinonen, A.V. Krasheninnikov, T. Thomson, A.K. Geim, I.V. Grigorieva, *Nature Physics* **8** 199 - 202 (2012)

[13] B.R.K. Nanda, M. Sherafati, Z.S. Popovic, S. Satpathy, *New Journal of Physics* **14** (2012)

[14] A.J.M. Giesbers, K. Uhlirova, M. Konecny, E.C. Peters, M. Burghard, J. Aarts, C.F.J. Flipse *Phys. Rev. Lett.* **111** 166101 (2013)

[15] Jeongmin Hong, Elena Bekyarova, Ping Liang, Walt A. de Heer, Robert C. Haddon, Sakhrat Khizroev *Scientific Reports* **2** 624 (2012)

[16] Zhiyong Wang, Chi Tang, Raymond Sachs, Yafis Barlas, Jing Shi *Phys. Rev. Lett.* **114** 016603 (2015)

[17] Kathleen M. McCreary, Adrian G. Swartz, Wei Han, Jaroslav Fabian, and Roland K. Kawakami *Phys. Rev. Lett.* **109** 186604 (2012)

[18] Elliott H. Lieb *Phys. Rev. Lett.* **62** 1201 (1989)

[19] J. J. Palacios and F. Yndurain *Phys. Rev. B* **85** 245443 (2012)

[20] G. N. Dash, Satya R. Pattanaik, Sriyanka Behera, *IEEE Journal of the Electron Devices Society* **2** 5 (2014)

[21] Electronic structure, Richard M. Martin (2004)

[22] P. Hohenberg, W. Kohn, *Phys. Rev.* **136** B864 (1964)

[23] U von Barth, L Hedin, *J. Phys. C: Solid State Physics* **5** (1972)

[24] N. David Mermin *Phys. Rev.* **137** A1441 (1965)

[25] W. Kohn, L.J. Sham ,*Phys. Rev.* **140** A1133 (1965)

[26] Density Functional Theory andthe Family of (L)APW-methods:a step-by-step introduction,S. Cottenier (2004)

[27] Pseudopotentials, Wikipedia.

[28] DFT in practice: Some "Fundae", Shobhana Narasimhan

CHAPTER 2

Impurity induced magnetism : functionalization

Although vacanices have been demostrated to produce magetic moments, controlling their formation remains a challenge as this requires us to manage the resultant stress[1]. Thus, functionalization is a better to create magnetic montents in graphene. In this chapter, we look at results obtained by functionalizing monolayer graphene. We start with a brief introduction detailing previous research and go on to present results obtained.

2.1 Background

Extensive studies have been done on functionalization of monolayer graphene by hydrogen, nitrogen, oxygen and fluorine. Yazyev et al. was among the first to perform this research and they reported a magnetic moment of $\approx 1.5\mu_B$ when distance between two chemisorbed hydrogen atoms is > 8.5 Å[2]. They also noted that two hydrogen induced moments in the same sublattice are ferromagnetically coupled, while those from different sublattices are anti - ferromagnetically coupled. Casolo et al. studied the adsorption of one, two, three and four hydrogen atoms and concluded that structures which minimize the lattice imbalance are favoured[3](i.e. structures where the number of adatoms on sublattice A and on sublattice B are not very different). Weigeng et al. showed that as the concentration of the hydrogen defects increases, the magnetic moment induced falls of rapidly, going down to zero at 5x5 supercells[4]. Zhou et al. theoretically predicted the stability of half hydrogenated graphene and it's ferromagnetic nature[5]. Several studies examined the effect of types of patterns on induced magnetic moment[6][7]. Yndurain examined the effect of hole doping on magnetic moment[8]. Sofo et al. carried out extensive studies on the single hydrogen adatom on graphene using a host of theoretical techniques[9], while Rudenko et al. studied the interaction between them[10].

Venezuela et al. cautioned about the use of single impurity doped unit cells in DFT due to long range nature of magnetic interactions[11]. Casolo et al. showed that the spin state for a single hydrogen chemisorbed on flat monolayer graphene $S_z = 0$ is wrong and this error can be attributed to self interaction error in DFT[12]. They suggested the use of hybrid functionals or GGA+U calculations to offset this problem, though the use of GGA+U gives erroneous results elsewhere. Kim et al. did a similar study for fluorine chemisorption[13].

There have been many experimental studies on this topic. Xie et al. observed room temperature ferromagnetism in partially hydrogenated epitaxial graphene[14]. McCreary et al. provided experimental evidence of magnetic moment formed by hydrogen adatoms by examining scattering of pure spin currents[15]. Hong et al. did similar studies for fluorine adatoms[16]. R.R. Nair et al. reported that fluorine chemisorption leading to paramagnetism[17]. Feng et al. studied the formation of magnetic moments by fluorine adatoms by fluorination of reduced graphene oxide[18].

2.2 Results and Discussion

2.2.1 Hydrogen

We reproduced the results obtained by Zhou et al.[5] for the half hydrogenate monolayer graphene. It has a total magnetic moment of 0.99 Bohr mag/cell and an absolute magnetic moment of 1.07 Bohr mag/cell. Relaxing the flat monolayer graphene with hydrogen distorts the planarity with the carbon atoms not attached to the hydrogen moving out of plane.

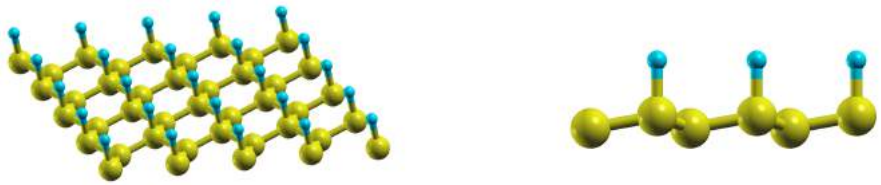

Figure 2.1: Structure of half hydrogenated graphene.

We then studied the effect of changing concentration of hydrogen adatoms on the

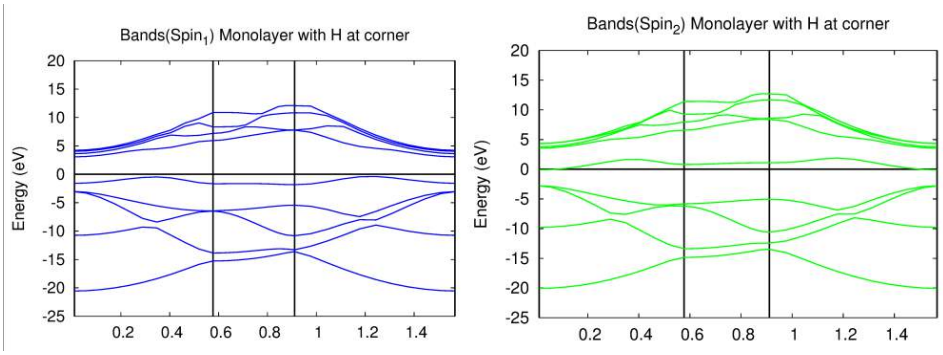

Figure 2.2: Band structure for both the spin polarizations.

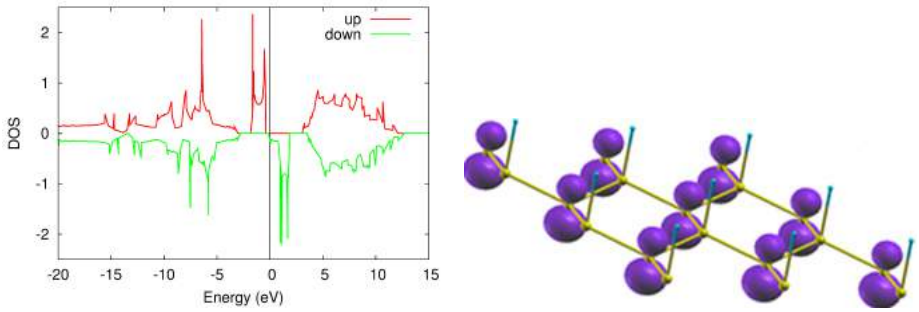

Figure 2.3: (Left)Density of states and (Right)Spin Iso-surface, note the concentraion of spin polarization on C-2, the carbon not attached to the hydrogen.

magnetic moment induced. The results are given in Table 3.1. Lowering the concentration of hydrogen adatoms lowers the induced magnetic moment. To confirm this hypothesis, we constructed supercells of sizes 1x1, 2x2, 4x4, 6x6.

Table 2.1: Size of supercell(In all cases, there is one hydrogen/supercell) vs magnetic moment.

Size of supercell	Total magnetization	Absolute magnetization
1x1	0.99	1.07
2x2	0.59	0.76
4x4	0.13	0.34
6x6	0.18	0.43

As suggested by Casolo et al.[12], we performed GGA+U calculations for the 6x6 supercell. Here U refers to the Hubbard U[19], a parameter which describes on site coulomb interactions.

Another calculation we performed was to construct supercells of 6x1, 6x2 and 6x3 size and place one hydrogen adatom at the center of each, and the results again showed

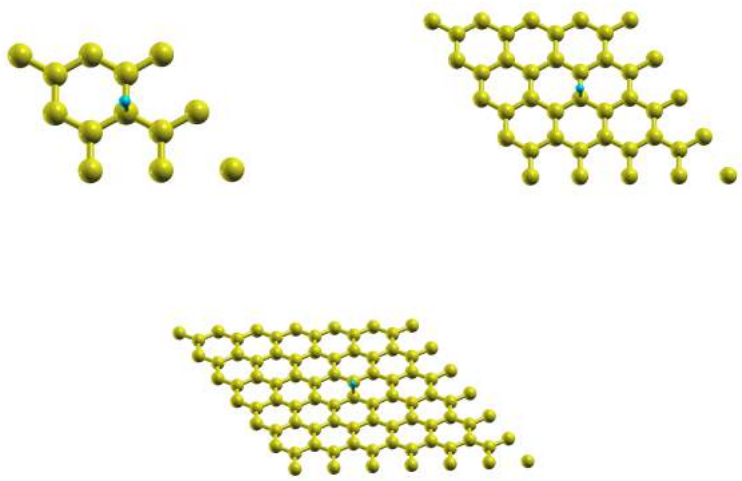

Figure 2.4: (Clockwise from top left)The 2x2, 4x4 and 6x6 supercells, each containing one hydrogen adatom at the center.

Table 2.2: Value of Hubbard U vd magnetic moment

Hubbard U	Total magnetization	Absolute magnetization
1	0.25	0.61
3	0.29	0.67
5	0.37	0.85
7	0.46	1.09
9	0.54	1.32

that lowering the concentration of hydrogen adsorbed lowers the induced magnetic moment.

Table 2.3: Size of supercell(In all cases, there is one hydrogen/supercell) vs magnetic moment.

Size of supercell	Total magnetization	Absolute magnetization
6x1	0.75	1.02
6x2	0.57	0.85
6x3	0.29	0.53

The hydrogen atoms were also placed above the monolayer right above the centres of the graphene hexagons, and they failed to induce any magnetic moment.

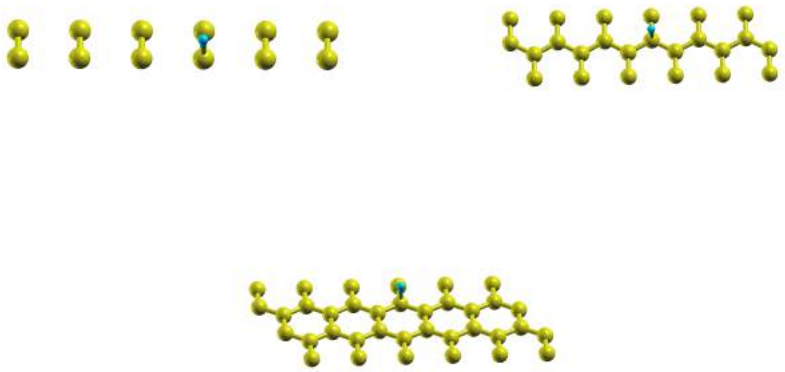

Figure 2.5: (Clockwise from top left)Asymmetric translation units of the 6x1, 6x2 and 6x3 supercells, each containing one hydrogen adatom at the center.

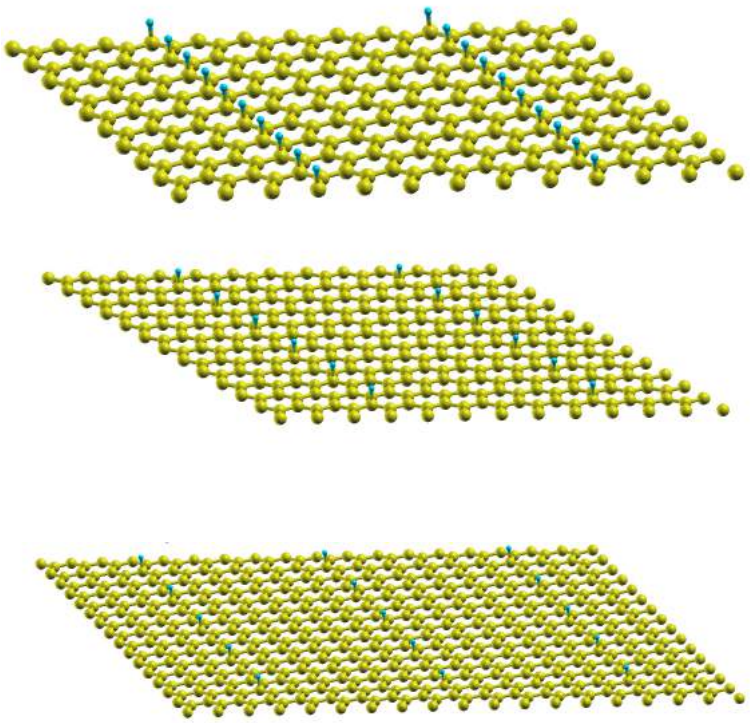

Figure 2.6: (Clockwise from top left)Extended view of the 6x1, 6x2 and 6x3 supercells.

2.2.2 Oxygen, Nitrogen and Fluorine

The relaxed structure of half nitrogenated monolayer graphene is similar to the half hyrogenated structure. But nitrogen fails to induce any magnetic moment. Neither does it do so when placed above the monolayer right above the centres of the graphene

The relaxed structure of half oxygenated monolayer graphene is similar to the half hyrogenated structure and oxygen adatoms induces a magnetic moment.

The relaxed structure of half fluorinated monolayer graphene is similar to the half hyrogenated structure and fluorine adatoms induces a magnetic moment.

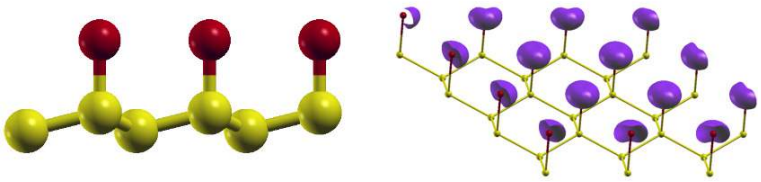

Figure 2.7: (Left) Relaxed structure of half oxygenated monolayer graphene, (Right) Isosurface of spin polarization, note that the concentration of spin polarization is higher at the oxygen atom than at the C2 carbon.

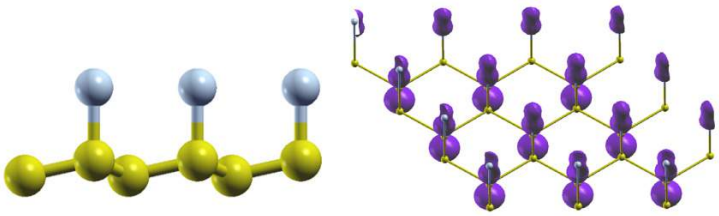

Figure 2.8: (Left) Relaxed structure of half fluorinated monolayer graphene, (Right) Isosurface of spin polarization, note that the concentration of spin polarization is higher at the C2 carbon than at the fluorine atom.

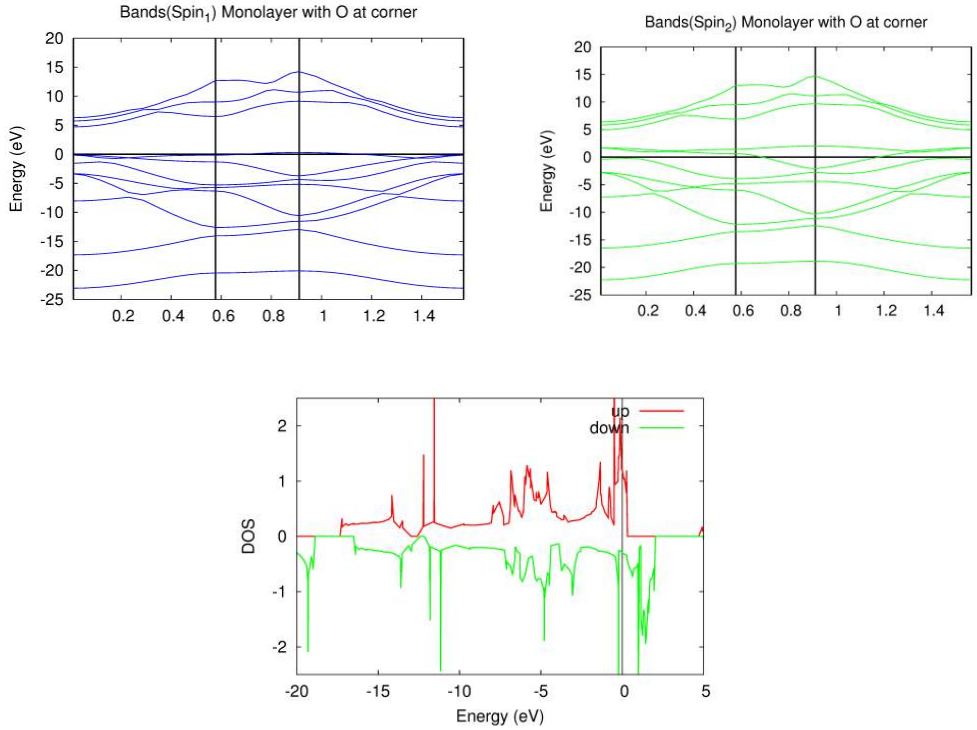

Figure 2.9: Band structure of half oxygenated monolayer graphene and Density of states.

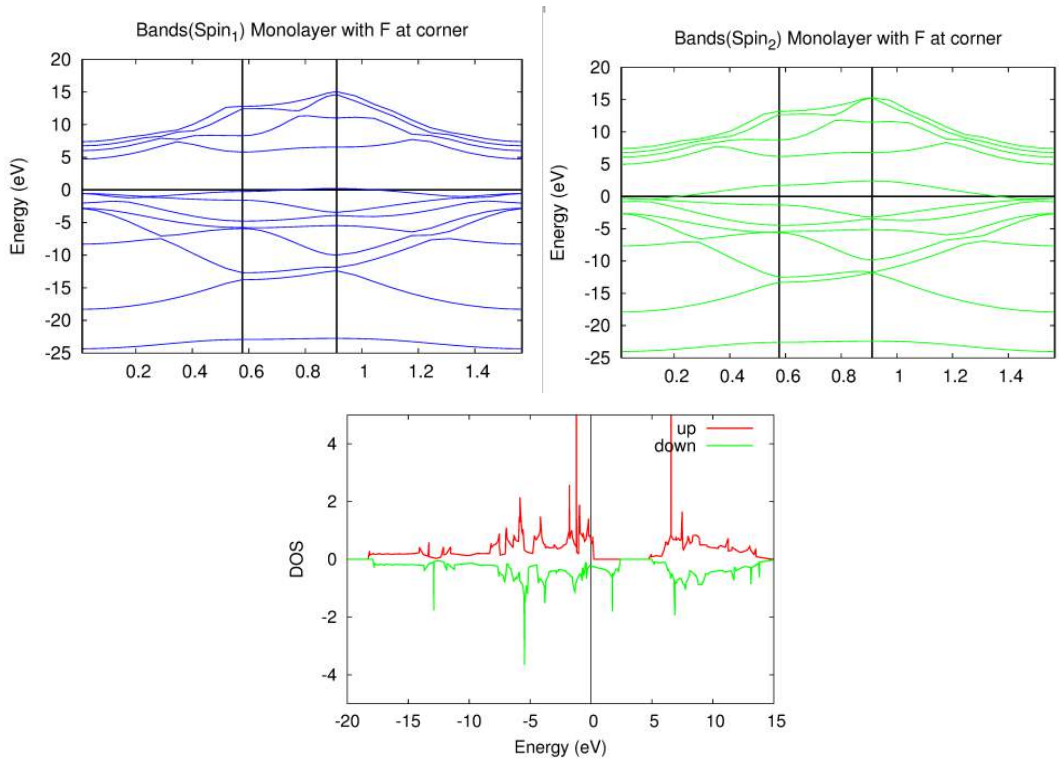

Figure 2.10: Band structure of half fluorinated monolayer graphene and Density of states.

REFERENCES

[1] Haricharan Padmanabhan, B. R. K. Nanda *Phys. Rev. B* **93** 165403 (2016)

[2] Oleg V. Yazyev, Lothar Helm *Phys. Rev. B* **75** 125408 (2007)

[3] Simone Casolo, Ole Martin Lovvik, Rocco Martinazzo, Gian Franco Tantardini *J. Chem. Phys.* **130** 054704 (2009)

[4] Weifeng Li, Mingwen Zhao, Yueyuan Xia, Ruiqin Zhangc, Yuguang Mu *J. Mater. Chem.* **19** 9274-9282 (2009)

[5] J. Zhou, Q. Wang, Q. Sun, X.S. Chen, Y. Kawazoe, P. Jena *Nano Lett.* **9** (11) 3867 - 3870 (2009)

[6] Ming Yang, Argo Nurbawono, Chun Zhang, Yuan Ping Feng, Ariando *Appl. Phys. Lett.* **96** 193115 (2010)

[7] J. Rivera-Julio, A.D. Hernandez-Nieves *Journal of Low Temperature Physics* **179** 1 (3 - 8) (2015)

[8] Felix Yndurain *Phys. Rev. B* **90** 245420 (2014)

[9] J.O. Sofo, Gonzalo Usaj, P.S. Cornaglia, A.M. Suarez, A.D. Hernandez-Nieves, C.A. Balseiro *Phys. Rev. B* **85** 115405 (2012)

[10] A.N. Rudenko, F.J. Keil, M.I. Katsnelson, A. I. Lichtenstein *Phys. Rev. B* **88** 081405(R) (2013)

[11] P. Venezuela, R.B. Muniz, A.T. Costa, D.M. Edwards, S.R. Power, M.S. Ferreira *Phys. Rev. B* **80** 241413(R) (2009)

[12] Simone Casolo, Espen Flage-Larsen, Ole Martin Lovvik, George R. Darling, Gian Franco Tantardini *Phys. Rev. B* **81** 205412 (2010)

[13] Hyun-Jung Kim, Jun-Hyung Cho *Phys. Rev. B* **87** 174435 (2013)

[14] Lanfei Xie, Xiao Wang, Jiong Lu, Zhenhua Ni, Zhiqiang Luo, Hongying Mao, Rui Wang, Yingying Wang, Han Huang, Dongchen Qi, Rong Liu, Ting Yu, Zexiang Shen, Tom Wu, Haiyang Peng, Barbaros Ozyilmaz, Kianping Loh, Andrew T.S. Wee1, Ariando, Wei Chen *Appl. Phys. Lett.* **98** 193113 (2011)

[15] Kathleen M. McCreary, Adrian G. Swartz, Wei Han, Jaroslav Fabian, and Roland K. Kawakami *Phys. Rev. Lett.* **109** 186604 (2012)

[16] X. Hong, K. Zou, B. Wang, S.-H. Cheng, J. Zhu *Phys. Rev. Lett.* **108** 226602 (2012)

[17] R.R. Nair, M. Sepioni, I-Ling Tsai, O. Lehtinen, J. Keinonen, A.V. Krasheninnikov, T. Thomson, A.K. Geim, I.V. Grigorieva *Nature Physics* **8** 199 - 202 (2012)

[18] Qian Feng, Nujiang Tang, Fuchi Liu, Qingqi Cao, Wenhai Zheng, Wencai Ren, Xiangang Wan, Youwei Du *ACS Nano* **7** (8) 6729 - 6734 (2013)

[19] Vladimir I. Anisimov, Jan Zaanen, Ole K. Andersen *Phys. Rev.B* **44** 943 (1991)

CHAPTER 3

Impurity induced magnetism : Intercalation

In this chapter, we look at results obtained by intercalating AA stacked bilayer graphene [1]. We start with a brief introduction detailing previous research and go on to present results obtained. Our electronic structure calculations show that when the center of the graphene hexagon coincides with the planar coordinates of the intercalated functional elements(H, N, O and F), the molecular behavior of these elements is lost and their atomic spin characters are retained for certain interlayer distances. As a consequence, unpaired electrons can be produced in these functionalized graphene layers.

In part 1 we will discuss electronic structure and magnetic properties of these intercalated systems. In part 2 we will discuss the results of stability analysis on the same. Finally, in part 3 we will discuss possible ways to overcome stability issues that have been highlighted in part 2.

3.1 Background

Intercalation of atoms and molecules between the layers of bilayer graphene as been studied extensively[1][2][3]. Their possible use for gas storage, separation, sensing etc has driven research into their properties[4]. Intercalating Calcium atoms between the layers of bilayer graphene makes it superconducting[5][6]. A magnetic transition was observed in ferric chloride intercalated bilayer graphene[7]. There have been studies carried out on C, N and O intercalation between bernal stacked layers of bilayer graphene[8].

[1]This cahpter has been presented at DAE Solid State Physics Symposium *AIP Conf. Proc.* **1731** 130040 (2016)

3.2 Computational and Structure Details

For the purpose of intercalation, we constructed two hexagonal (AA) stacked graphene layers with variable interlayer distance and intercalated the considered functional elements (H, N, O and F) at the hollow site as shown and described in Fig. 1. Since the layers are infinite in the plane, we considered a single unit cell of graphene in each layer and allowed the Bloch periodicity. Also as we have assumed complete intercalation, there is a suspended functional layer with hexagonal lattice geometry as can be seen from Fig. 1 (right). Altogether the considered composite unit cell has four carbon atoms and one functional element.

Density functional calculations were carried out on the composite unit cell using pseudopotential approximation and plane wave basis set as implemented in Quantum Espresso[9]. The kinetic energy cut off was taken as 30 Ry. The Brillouin zone integration was performed out using tetrahedron method for a 25x25x2 k-mesh. The ground state was obtained using GGA exchange-correlation functional[10] and Vanderbilt ultra-soft pseudopotentials[11].

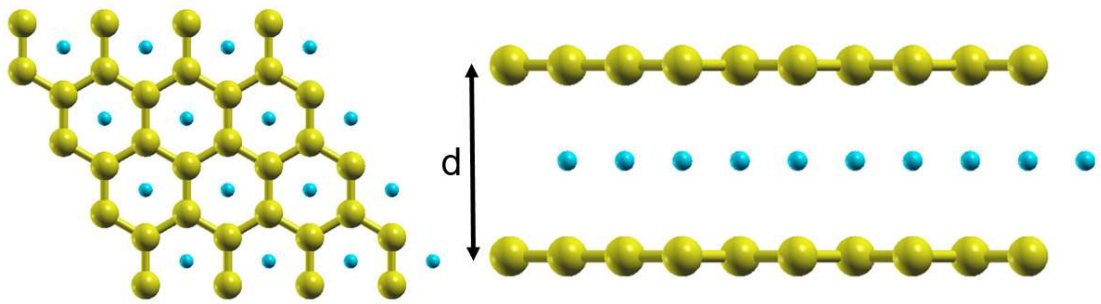

Figure 3.1: (Right)Two hexagonal (AA) stacked graphene layers with intercalated functional elements represented in blue. Here, d represents the interlayer distance. The functional elements are kept at equidistance from both the layers. (Left) The top view of the composite showing the matching between the planar coordinate of the functional element and the centre of the graphene hexagon. Conventionally this planar position is referred as the hollow site.

3.3 Results and Discussion : Part 1

In Fig. 2 we have plotted the total energy and magnetization of the intercalated graphene for the functional elements considered in this work. For H and N intercalation the sys-

tem is magnetized when the interlayer distance d is between 4 to 5Å. The total energy plotted in Fig. 2 (left) indicates that through this intermediate region the system makes a transition from the completely unstable state to a stable state. In the case of O and F intercalation, the system gets magnetized for multiple ranges of d. While smaller value of d is energetically unfavorable, the system gains stability when d goes beyond 5Åsuggesting the practical realization of magnetism in intercalated graphene. For the H and N, even though the range of d for which the magnetization arises is not a stable phase, external pressure can be applied to synthesize the desired structure.

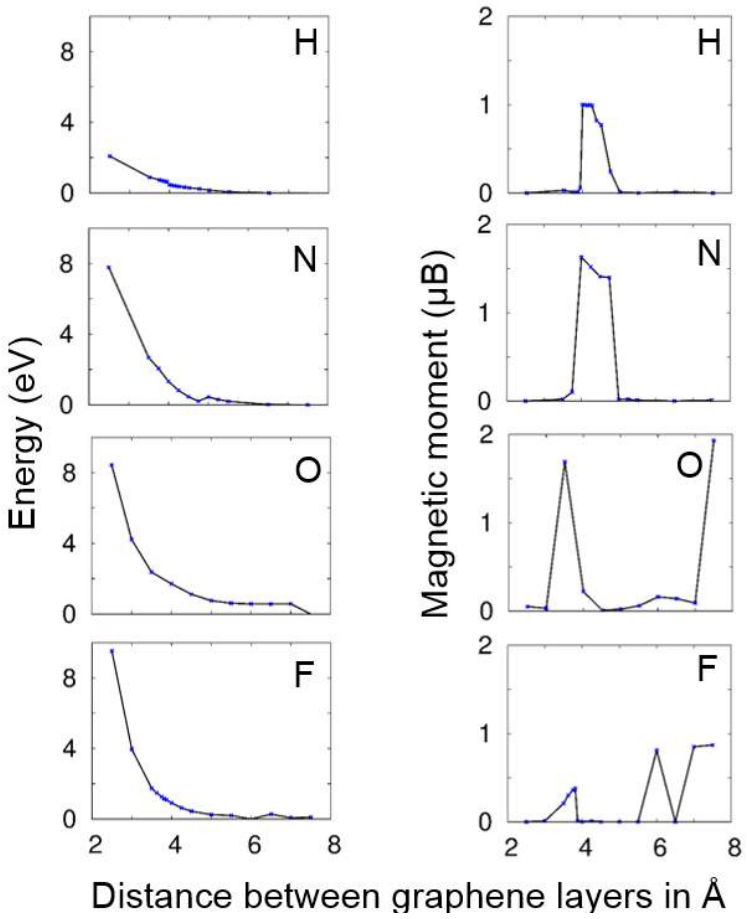

Figure 3.2: Total energy (left) and magnetization (right) as a function of interlayer distance for the intercalated graphene with different functional elements.

To gain insight to the origin of magnetizaion we have plotted the spin-density of these intercalated systems in Fig. 3. The figure suggests that the graphene layers remain non-magnetic. However, they ensure the spin-polarization of the valence electrons of the functional elements. For H, the spin-density takes the shape of the 1s wavefunction indicating that a spin-half state is formed. For N, O and F, we have respectively 3, 4 and

5 electrons available to occupy the outer 2p states. Therefore, with high-spin(HS) the complete spin-polarization would yield 3, 2 and $1\mu B$ magnetic moment for N, O and F respectively. The results shown in Fig. 2 adhere to the HS state for O and F. However, magnetization for N intercalated system results with an intermediate spin state. The shape of the spin-density for N and F indicates immediate spin-polarization of the valence pz state.

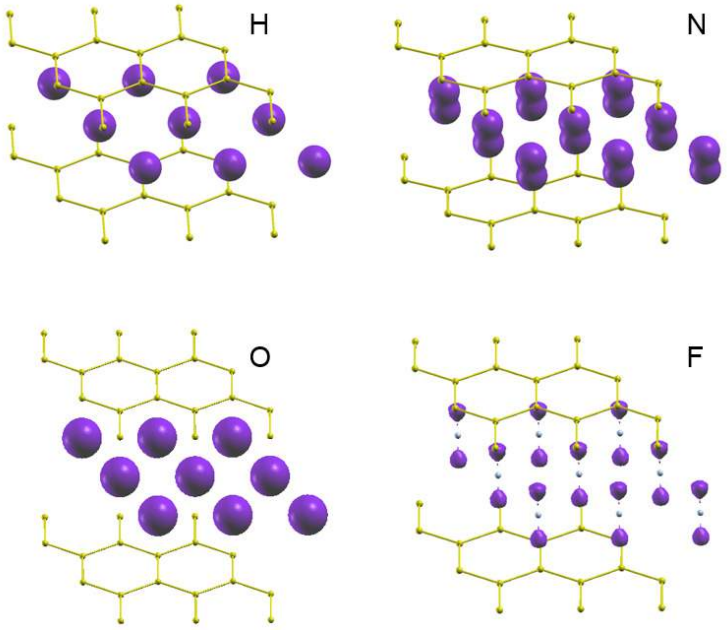

Figure 3.3: The spin density of H, N, O and F intercalated graphene. While the graphene layers are not spin-polarized they ensure the polarization of the valence electrons of the functional elements.

To understand the relation between magnetization and interlayer separation, in Fig. 4, we have plotted the spin-resolved band structure for H intercalated graphene for three different d values. Similar band-structures are obtained for other intercalated systems, but not presented here to avoid redundancy. The basic features of the band structures, shown in the figure, include regular graphene π bands and the presence of the H-1s state in the form of an additional dispersed band. The dispersion happens as the intercalated H forms a hexagonal lattice for itself (see Fig. 1). When the interlayer distance is very small or very large this 1s state is equally occupied in both the spin channels to stabilize in a non-magnetic ground state. For an intermediate separation (4Å< d < 5Å), the 1s state is occupied in one spin channel and keeping the other spin channel empty due to non-availability of electrons.

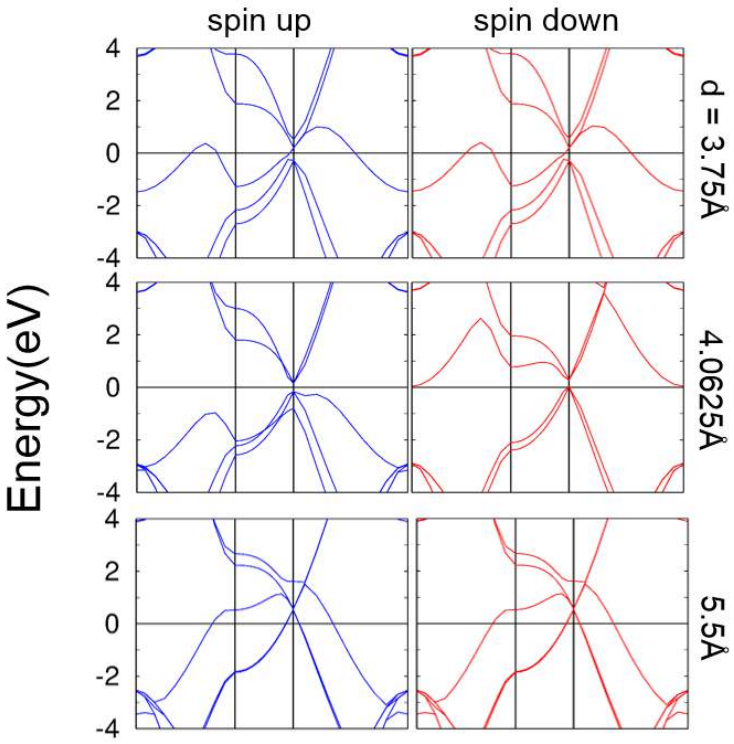

Figure 3.4: The spin-resolved band structure for hydrogen intercalated graphene with different interlayer separations

Primarily the graphene layers provide a one-dimensional confinement potential V to the valence electrons of the functional elements. The confinement potential acts as perturbation to the original Hamiltonian involving the kinetic energy and spin-exchange energy components. For certain V, the spin-exchange component lowers the energy to favor a magnetic ground state.

REFERENCES

[1] Donghui Guo, Takahiro Kondo, Takahiro Machida, Keigo Iwatake, Susumu Okada, Junji Nakamura *Nature Communications* **3** 1068 (2012)

[2] James Kleeman, Katsuaki Sugawara, Takafumi Sato, Takashi Takahashi *J. Phys. Soc. Jpn.* **83** 124715 (2014)

[3] K. Sugawara, K. Kanetani, T. Sato, T. Takahashi *AIP Advances* **1** 022103 (2011)

[4] K. Rohini, Daniel M.R. Sylvinson, R.S. Swathi *J. Phys. Chem. A* **119** (44) 10935 - 10945 (2015)

[5] S.L. Yang, J.A. Sobota, C.A. Howard, C.J. Pickard, M. Hashimoto, D.H. Lu, S.K. Mo, P.S. Kirchmann, Z.X. Shen *Nature Communications* **5** 3493 (2014)

[6] E. R. Margine, Henry Lambert, Feliciano Giustino *Scientific Reports* **6** 21414 (2016)

[7] Namdong Kim, Kwang S. Kim, Naeyoung Jung, Louis Brus, Philip Kim *Nano Lett.* **11** (2) 860 - 865 (2011)

[8] S.J. Gong, W. Sheng, Z.Q. Yang and J.H. Chu *Journal of Physics: Condensed Matter* **22** 24 (2010)

[9] Paolo Giannozzi, Stefano Baroni, Nicola Bonini, Matteo Calandra, Roberto Car, Carlo Cavazzoni, Davide Ceresoli, Guido L Chiarotti, Matteo Cococcioni, Ismaila Dabo, Andrea Dal Corso, Stefano de Gironcoli, Stefano Fabris, Guido Fratesi, Ralph Gebauer, Uwe Gerstmann, Christos Gougoussis, Anton Kokalj, Michele Lazzeri, Layla Martin-Samos, Nicola Marzar, Francesco Mauri, Riccardo Mazzarello, Stefano Paolini, Alfredo Pasquarello, Lorenzo Paulatto, Carlo Sbraccia, Sandro Scandolo, Gabriele Sclauzero, Ari P Seitsonen, Alexander Smogunov, Paolo Umari, Renata M Wentzcovitch *Journal of Physics: Condensed Matter* **21** 39 (2009)

[10] David Vanderbilt *Phys. Rev. B* **41** 7892(R) (1990)

[11] John P. Perdew, Kieron Burke, Yue Wang *Phys. Rev. B* **54** 16533 (1996)

[12] Yichen Jia, Huan Zhao, Qiushi Guo, Xiaomu Wang, Han Wang, Fengnian Xia *ACS Photonics* **2** (7) 907 - 912 (2015)

[13] Qiucheng Li, Mengxi Liu, Yanfeng Zhang, Zhongfan Liu *Small* **12** (1) 32 - 60 (2016)

[14] Jun Hua Meng, Xing Wang Zhang, Hao Lin Wang, Xi Biao Ren, Chuan Hong Jin, Zhi Gang Yin, Xin Liua, Heng Liua *Nanoscale* **7** 16046 - 16053 (2015)

[15] Yoshiyuki Miyamoto, Hong Zhang, Takehide Miyazaki, Angel Rubio *Phys. Rev. Lett.* **114** 116102 (2015)

CHAPTER 4

Force calculations and suggestions for stabilizing the intercalated atom

We have shown in the last chapter that by intercalating H, N, O and F atoms in bilayer graphene and by suitably adjusting the interlayer distance, we can create local magnetic moments. In this chapter we will study the stability of the above mentioned systems. To do this, we plot the force at every point inside the hexagon. We then suggest that another layer of atoms be inserted between the graphene layers to make the intercalated atom stable at the center.

4.1 Stability analysis for intercalated atoms

4.1.1 Hydrogen

We calculated the energy of the system with hydrogen atom at the center and hydrogen atom at the corner with both GGA and vDW pseudopotentials.

Table 4.1: Energy of system with hydrogen at different positions in Ry

Type of pseudopotential	Center	Corner
GGA	-46.55663830	-46.59172796
vDW	-46.86135894	-46.91118270

The force at each point was found out and plotted to get a clearer picture. The force plot for hydrogen atom at (x,y) co-ordinates is given below (note that along the z axis, the impurity atom always lies in the plane exactly in between the two graphene layers). The above table and the plot below make it abundantly clear that the hydrogen atom is not stable at the center of the hexagon. The forces are homogeneous except for a few points.

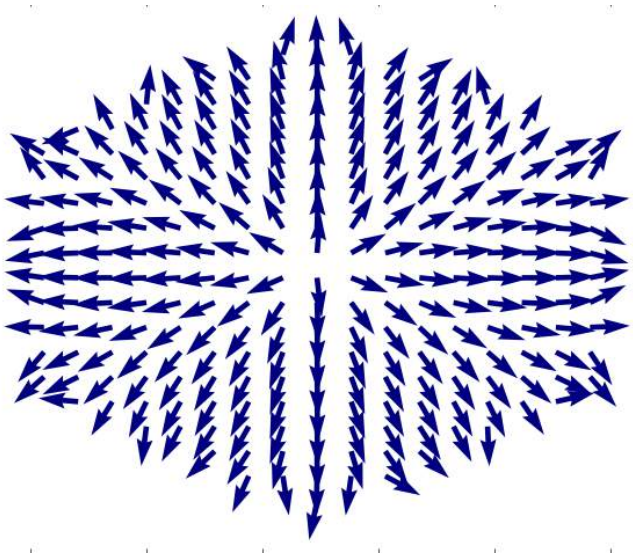

Figure 4.1: Each arrow represents the direction of force felt by the hydrogen atom.

4.1.2 Nitrogen

As is the case with the hydrogen atom, the nitrogen atom is also unstable at the center.

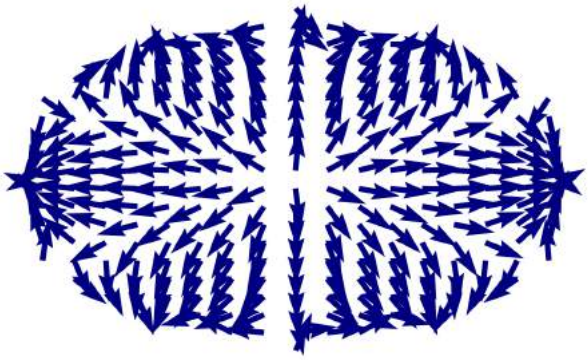

Figure 4.2: Force plot for N where each arrow represents the direction of force felt by the impurity atom.

4.1.3 Oxygen

When the bilayer graphene is intercalated with oxygen atoms, magnetism is induced at two distances, 3.5Å and 7.5Å. The force at both distances was plotted. The oxygen atom is unstable in both the cases.

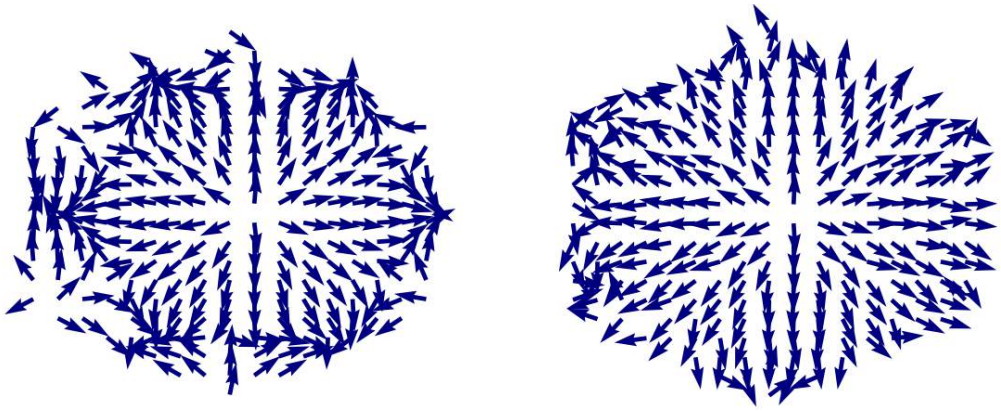

Figure 4.3: (Left)Force plot at 3.5 Å(Right) Force plot at 7.5 Åfor the oxygen impurity atom

4.1.4 Fluorine

When the bilayer graphene is intercalated with fluorine atoms, magnetism is induced at two distances, 3.81Å and 6.0Å. The force at both distances was plotted. The fluorine atom is unstable at 3.81Å, but it is stable at 6.0Å.

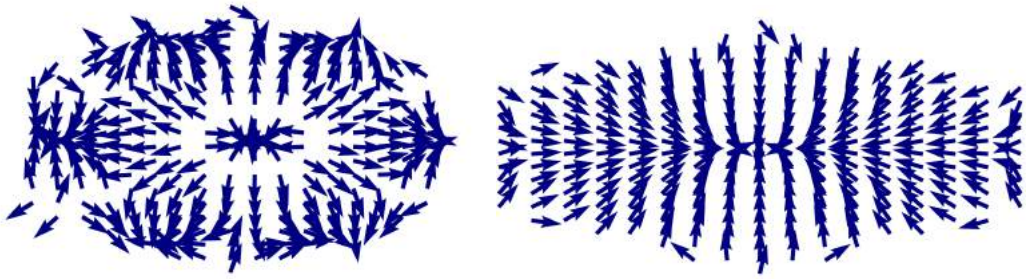

Figure 4.4: (Left)Force plot at 3.8125 Å(Right) Force plot at 6.0 Åfor the fluorine impurity atom

4.1.5 Other atoms tested

We also intercalated other atoms to see if they did induce magnetism. We tested with Li, Be, B, Na, Al, Si, P, S, Cl, Br and I. Of these, only sulphur and chlorine induced a magnetic moment, however they were unstable.

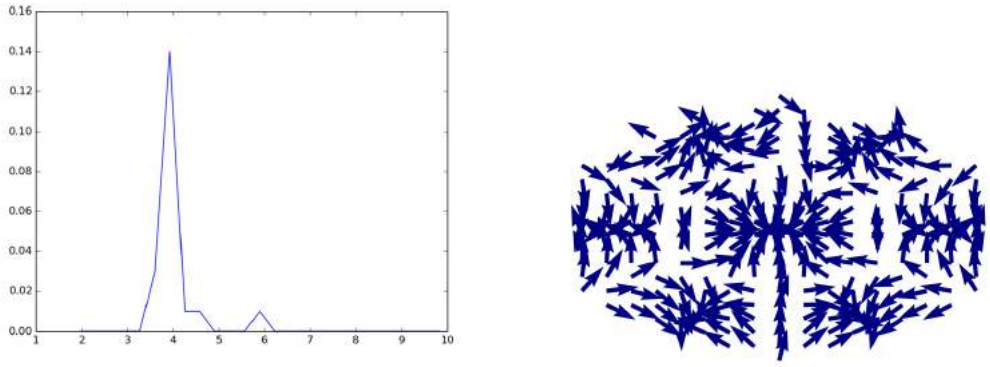

Figure 4.5: Plot of magnetic moment induced in Bohr mag/cell vs distance between the graphene layers in Åand force plot for Chlorine.

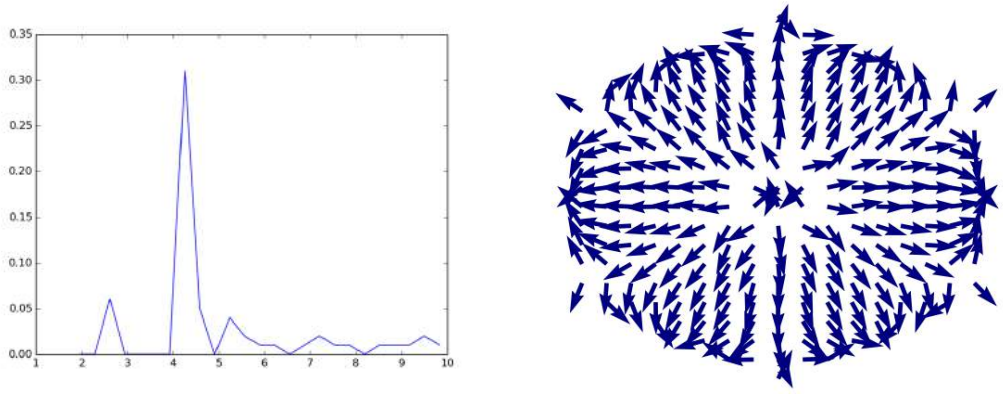

Figure 4.6: Plot of magnetic moment induced in Bohr mag/cell vs distance between the graphene layers in Åand force plot for Sulphur.

4.2 Stability analysis with added midlayer

To stabilize the intercalated atom, we added a third layer in between the two graphene layers. In the following subsections, we discuss the results obtained.

4.2.1 Carbon atom midlayer

In this case, we added a layer of carbon atoms in between the two graphene layers. This is the familiar trilayer graphene. The results for the intercalation of H, N, O and F atoms are presented below.

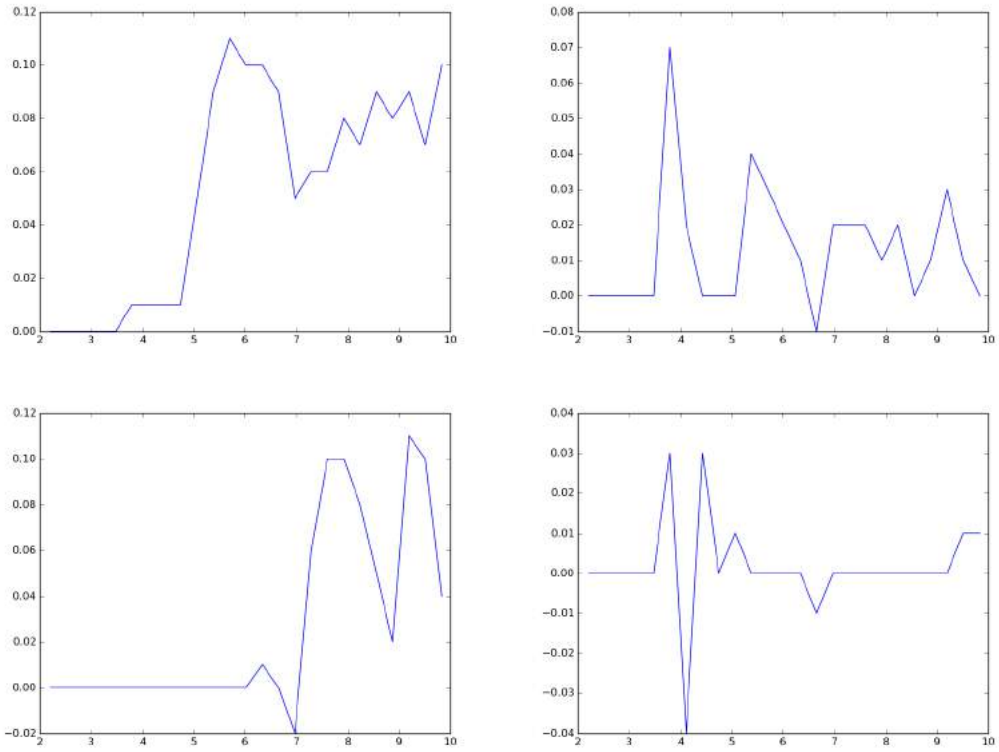

Figure 4.7: (Clockwise from top left) Plots of magnetic moment induced in Bohr mag/-cell vs distance between the graphene layers in Åfor trilayer graphene intercalated with H, N, O and F.

We can see that the magnitude of induced moment is very low. Below are the spin polarization plots for H and F intercalation. These plots confirm that it is indeed the intercalated atoms which are spin polarized.

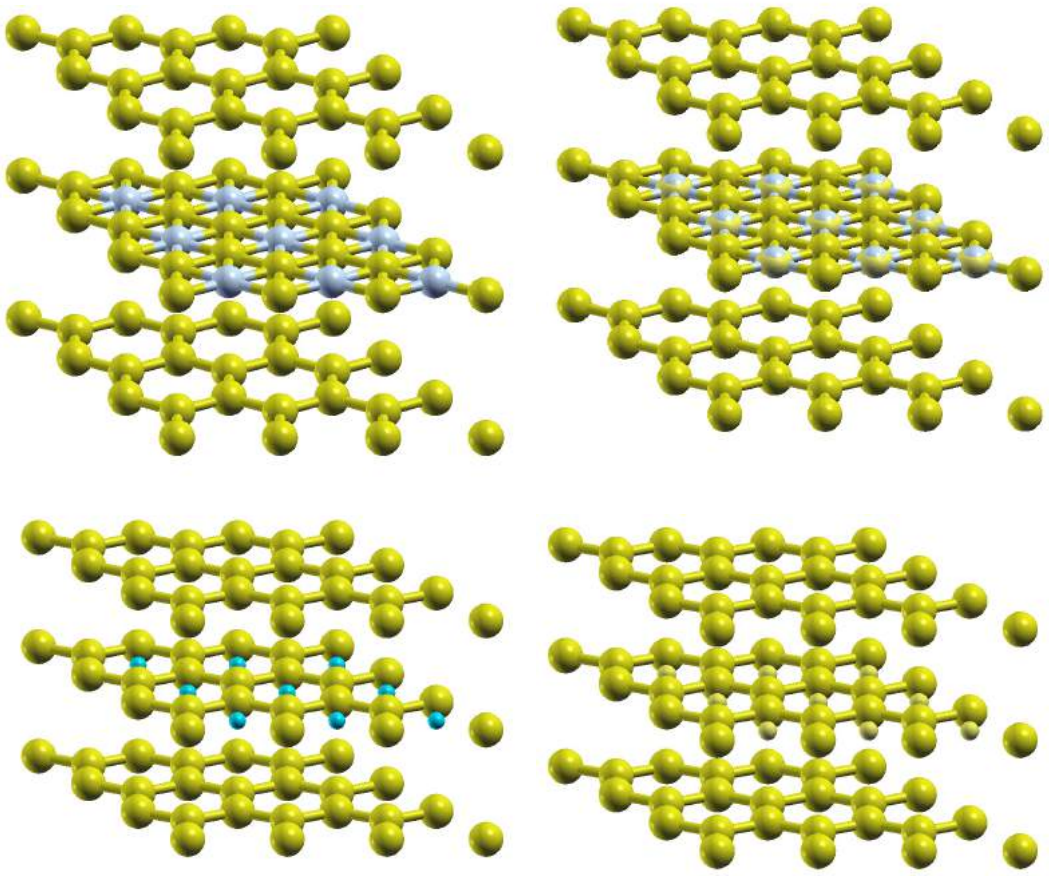

Figure 4.8: (Top row) Structure and spin polarization plot of Fluorine intercalation in trilayer graphene, (Bottom row) Structure and spin polarization plot of Hydrogen intercalation in trilayer graphene

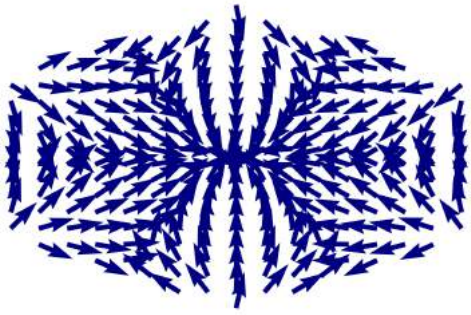

Figure 4.9: Force plot for hydrogen atom intercalated in trilayer graphene.

4.2.2 Hydrogen atom midlayer

In this case, we added a layer of hydrogen atoms in between the two graphene layers to stabilize the intercalated atom. The hydrogen atoms are placed at the mid point of the carbon atoms, thus forming a graphene like layer. The results for the intercalation of H, N, O and F atoms are presented below.

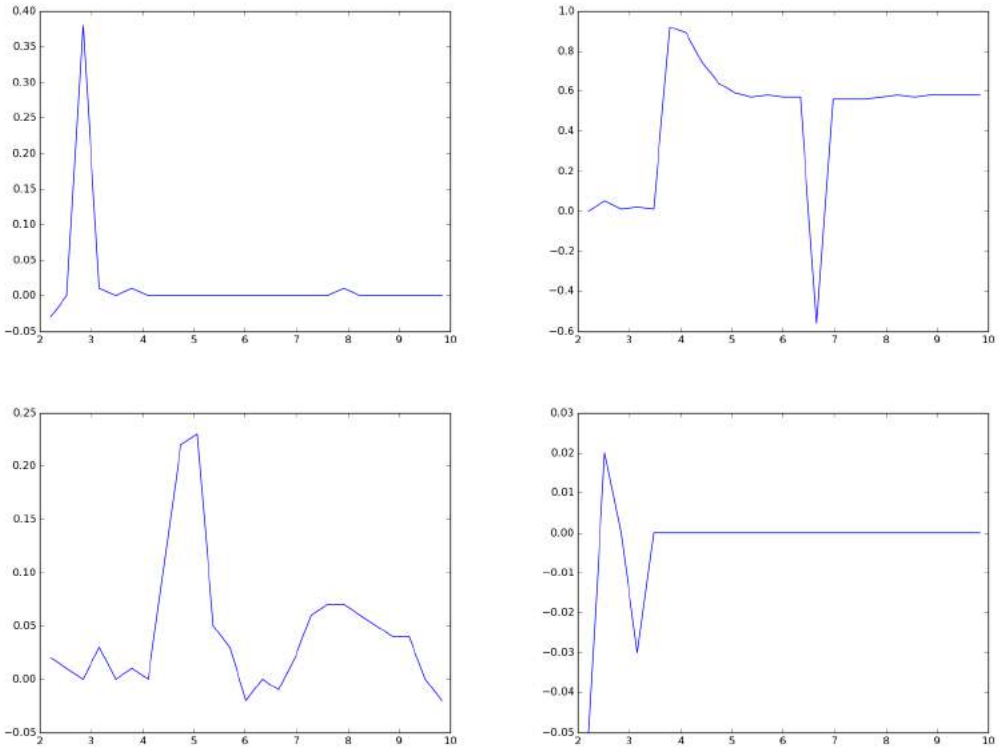

Figure 4.10: (Clockwise from top left) Plots of magnetic moment induced in Bohr mag/cell vs distance between the graphene layers in Åfor bilayer graphene with a midlayer of hydrogen atoms intercalated with H, N, O and F.

The spin polarization plots for hydrogen confirmed that it was the intercalated hydrogen atom that was polarized, though at a very small interlayer distance. A force plot shows that the hydrogen atoms are stable.

The spin polarization plots for fluorine however showed that the fluorine atoms were not getting polarized, but the hydrogen atoms were.

The spin polarization plots for nitrogen intercalation reveal that the nitrogen atoms do get polarized, except for one case when the indued moment is negative. However, the force plots reveal that the nitrogen atom is unstable at the center even after adding hydrogen atoms to stabilize it.

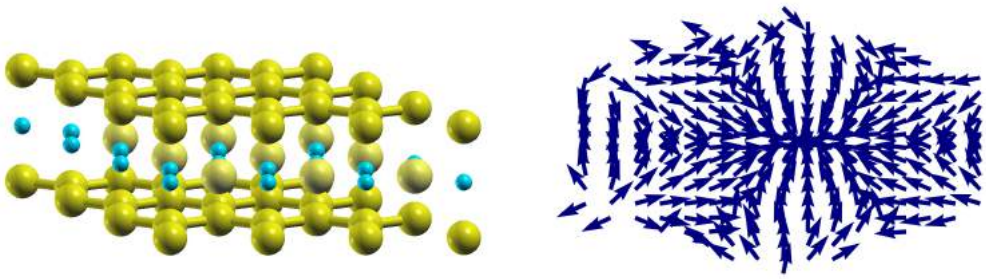

Figure 4.11: Spin polarization and force plot for bilayer graphene with a midlayer of hydrogen atoms intercalated with H

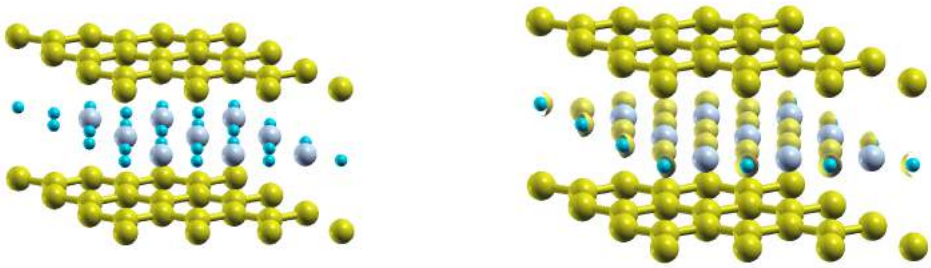

Figure 4.12: Structure and spin polarization plot for bilayer graphene with a midlayer of hydrogen atoms intercalated with H

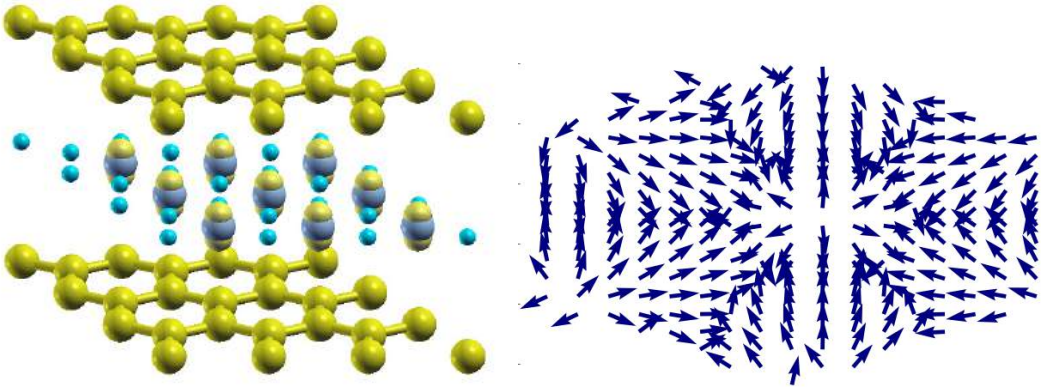

Figure 4.13: Spin polarization and force plot for bilayer graphene with a midlayer of hydrogen atoms intercalated with N

4.2.3 Hexa-Boron Nitride midlayer

In this case, we added a layer of hexa boron nitride in between the two graphene layers (AAA stacking). The results for the intercalation of H, N, O and F atoms are presented below.

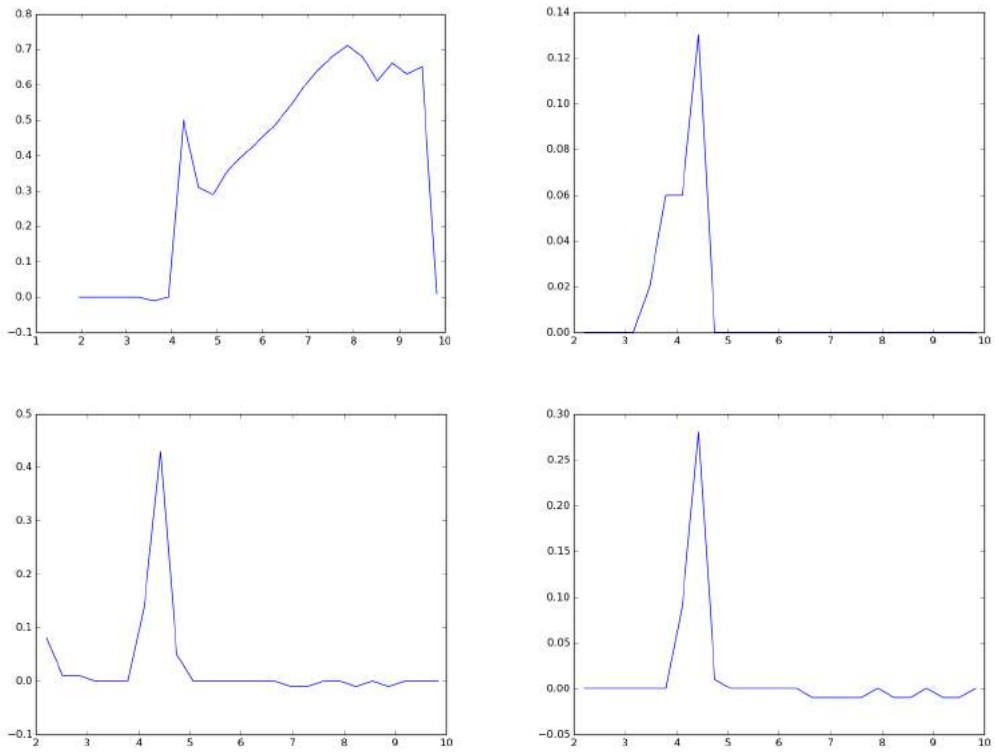

Figure 4.14: (Clockwise from top left) Plots of magnetic moment induced in Bohr mag/cell vs distance between the graphene layers in Åfor bilayer graphene with a midlayer of hexa-BN intercalated with H, N, O and F.

At around 4 Åinter layer distance(between the graphene layers) the systems becomes magnetic irrespective of which atom is intercalated. Spin polarization plots however reveal that the carbon atoms in the graphene get polarized and not the intercalated atom.

When intercalated with H atoms, the systems reamins magnetic even for larger interlayer distances. The spin polarization plot at these distances reveal that hydrogen atoms get polarized. Force plots show that the intercalated hydrogen atoms are stabe at the center.

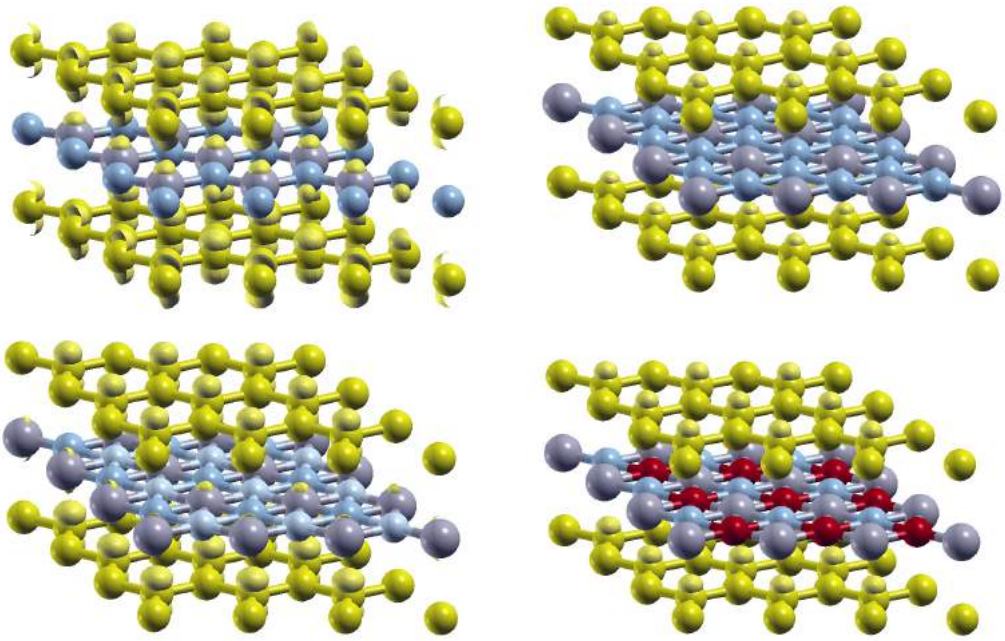

Figure 4.15: (Clockwise from top left) Spin polarization plots for bilayer graphene with a midlayer of hexa-BN intercalated with H, N, O and F (at first magnetization peak).

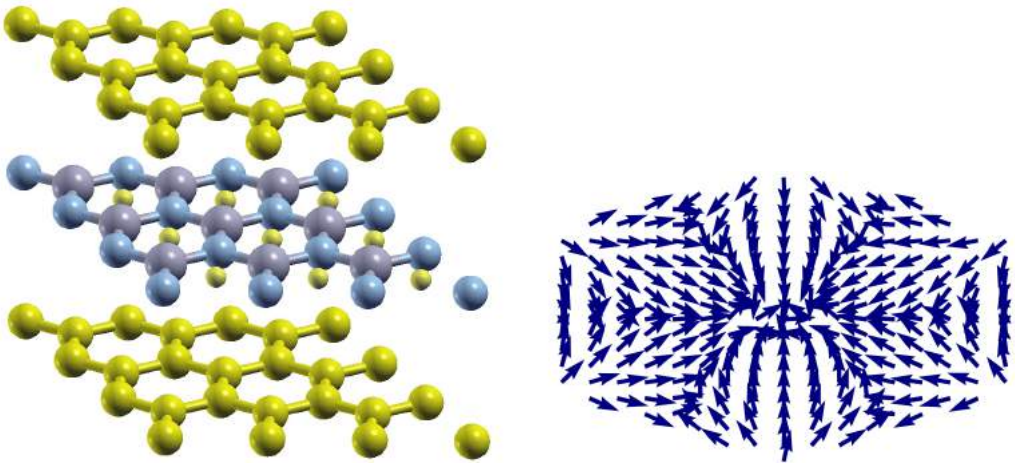

Figure 4.16: Spin polarization plots for bilayer graphene with a midlayer of hexa-BN intercalated with H at large interlayer distance and force plot of the same.

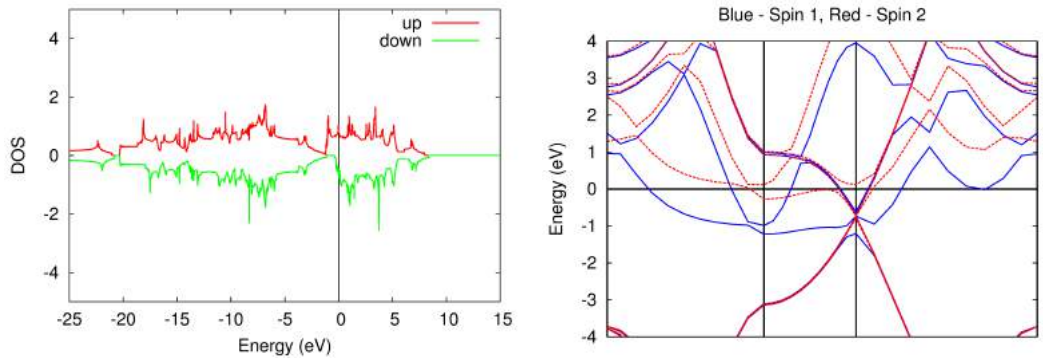

Figure 4.17: Desity of states and band structure for bilayer graphene with a midlayer of hexa-BN intercalated with H at large interlayer distance and force plot of the same.

4.3 Conclusion

Thus, we have seen that addition of a midlayer enhances the stability of the intercalated atom while preserving the magnetic moment formed. Adding a layer of hexa - boron nitride stabilizes the hydrogen at the center of the hexagon and preserves the magnetic moment. At large interlayer distance(6Å), the intercalated fluorine atom gives rise to magnetic moment and is also stable without any midlayer.

APPENDIX A

Code 1 : Python code to create the input files for stress calculation.

```
# -*- coding: utf-8 -*-
"""
Created on Wed Jan 20 15:29:58 2016

@author: sajid
"""

from numpy import*
from scipy import*
from numpy.linalg import*
from matplotlib.pyplot import*
from matplotlib.path import*

x = linspace(-2,3,35)
y = linspace(-2,3,35)
z = meshgrid(x,y)
A = append(z[0].reshape(-1,1),z[1].reshape(-1,1),axis=1)
C = A.copy()
p1 = array([[0.0000000000,0.0000000000] , [0.0000000000,1.4179725000
p = Path(p1)
b = where(p.contains_points((A)))
points = A[b]
#scatter(points[:,0],points[:,1])
print len(points)
points = array(points)
```

```
a = 2.456001395
points[:,1] = points[:,1] * (2.0/sqrt(3)) * (1.0/a)
points[:,0] = ( points[:,0] - points[:,1] * (-a/2.0) ) * (1.0/a)

#points[:,1] = points[:,1] % 1
#points[:,0] = points[:,0] % 1

pos = points
pos = array(pos)
pos[:,0] = points[:,0] * a + points[:,1] * (-a/2.0)
pos[:,1] = points[:,1] * (2.456/2.0) * sqrt(3)
scatter(pos[:,0],pos[:,1])



for i in range(len(points)):
    a = open('temp.scf.in','r')
    b = a.readlines()
    j = str(i)
    b[4] = "\t\t      outdir = '/home/physics/Documents/Sajid/Stress
    b[34] = 'H    '+str(points[i][0])+'    '+str(points[i][1])+'
0.19494701445\n'
    c = open('case_number'+str(i)+'.scf.in','w')
    c.writelines(b)
    c.close()
```

APPENDIX B

Code 2 : Python code to plot the output of stress calculations.

```
# -*- coding: utf-8 -*-
"""
Created on Sat Jan 23 16:10:18 2016

@author: physics
"""

from numpy import*
from scipy import*
from numpy.linalg import*
from matplotlib.pyplot import*
from mpl_toolkits.mplot3d import axes3d

data = []
pos  = []

ncalc = 244

for i in range(ncalc):
    a = open('case_number'+str(i)+'.scf.out','r')
    b = a.readlines()
    for j in range(len(b)) :
        if b[j] == '   Cartesian axes\n' :
            pos_temp=[]
            pos_temp.append(b[j+7].split())
            pos.append(array(map(float,pos_temp[0][-4:-1]))*2.456001
```

```
            if b[j] ==    '     Forces acting on atoms (Ry/au):\n' :
                temp = []
                temp.append(map(float,b[j+2].split()[-3:]))
                temp.append(map(float,b[j+3].split()[-3:]))
                temp.append(map(float,b[j+4].split()[-3:]))
                temp.append(map(float,b[j+5].split()[-3:]))
                temp.append(map(float,b[j+6].split()[-3:]))
        data.append(temp)
pos = array(pos)

force_tot = []
force_x   = []
force_y   = []

for i in range(ncalc):
    x = pos[i][0]
    y = pos[i][1]
    f_x = data[i][-1][0]
    f_y = data[i][-1][1]
    force_x.append(f_x)
    force_y.append(f_y)
    force = sqrt(f_x**2 + f_y**2)
    force = force * 10**5
    force_tot.append(force)
    #j = range(50)
    quiver(x,y,f_x,f_y,force)
    #title('%d * 10^(-5)' % force)
    xlim(-0.3,2.8)
    ylim(-1.0,2.3)
    #savefig('plot_number = i'+str(l)+'.png')
    #clf()
#quiver(pos[:,0],pos[:,1],force_x,force_y)
```

show ( )

LIST OF PAPERS BASED ON THESIS

1) Magnetism in Intercalated Graphene, Sajid Ali, Ranjit Nanda *60th DAE Solid State Physics Conference* 21 - 25 December 2015. *AIP Conf. Proc.* **1731** 130040 (2016)

2) Magnetism in Graphene, Haricharan Padmanabhan, Azad Amitoz, Sajid Ali, Ajit Jena, Ranjit Nanda, Poster Presentation at *Workshop on The Physics and Chemistry of Graphene and Other Single and Bilayer Materials Including* MoS_2 *and Phosphorene* Dec 2014.